### Title

Single phonon detection for dark matter via quantum evaporation and sensing of He3




### Journal

Physical Review D, 109(2)

### ISSN

2470-0010



### Authors

Lyon, SA

Castoria, Kyle

Kleinbaum, Ethan

et al.



### Publication Date

2024-01-15

### DOI

10.1103/physrevd.109.023010

# Single Phonon Detection for Dark Matter via Quantum Evaporation and Sensing of $^3$Helium

S. A. Lyon, Kyle Castoria and Ethan Kleinbaum*
*Department of Electrical and Computer Engineering, Princeton University, Princeton, NJ 08544*

Zhihao Qin, Arun Persaud, Thomas Schenkel
*Acceleration Technology & Applied Physics, Lawrence Berkeley National Laboratory, 1 Cyclotron Road, CA 94720, USA*

Kathryn M. Zurek
*Walter Burke Institute for Theoretical Physics, California Institute of Technology, Pasadena, CA 91125*

Dark matter is five times more abundant than ordinary visible matter in our Universe. While laboratory searches hunting for dark matter have traditionally focused on the electroweak scale, theories of low mass hidden sectors motivate new detection techniques. Extending these searches to lower mass ranges, well below $1\,\mathrm{GeV/c^2}$, poses new challenges as rare interactions with standard model matter transfer progressively less energy to electrons and nuclei in detectors. Here, we propose an approach based on phonon-assisted quantum evaporation combined with quantum sensors for detection of desorption events via tracking of spin coherence. The intent of our proposed dark matter sensors is to extend the parameter space to energy transfers in rare interactions to as low as a few meV for detection of dark matter particles in the keV/c$^2$ mass range.

Dark matter (DM) direct detection experiments have focused on detecting Weakly Interacting Massive Particles (WIMPs) via nuclear recoils (see *e.g.* Ref. [1] for a review), where DM with mass in the 100 GeV range deposits energy by elastic scattering. However, in theories with low-mass hidden sectors (called a hidden valley), thermal DM can be much lighter, even down to a keV in mass where it carries meV of kinetic energy ($\frac{1}{2}m_X v_X^2$, with $v_X \simeq 10^{-3}c$). As the mass of the DM drops below approximately 10 GeV, the detection of rare scattering events with target nuclei falls below detection thresholds, and target nuclei absorb a very small fraction of the DM kinetic energy; see Ref. [2] for a review. At lower energies, electron recoils with energy transfer thresholds in the 1 eV range can be detected with sensitive charge coupled devices (CCD) counting electron-hole pairs in semiconductors, (*e.g.* [3]) or athermal phonon detectors (*e.g.* [4]). However, dark matter events have not yet been observed in these energy ranges, and it is desirable to probe thermal DM as light as 1 keV. Thus developing systems which can detect rare events with even lower deposited energy is an important goal.

In solids and liquids the lower energy excitations are generally phonons [5] (and rotons in superfluid helium [6, 7]). Ionic crystals (polar materials) are especially interesting as detectors, since they enable new pathways for interaction with DM [5, 8–10]. One challenge to sensing these phonons is that they are itinerant. Initially generated optical phonons rapidly decay to acoustic phonons, which disperse the deposited energy throughout the detection medium. The development of very sensitive and optimized detectors for quasiparticles and phonons using transition edge sensors (TES) and superconducting nanowire detectors (SNSPD) is underway [11].

Here we propose an alternative, novel detection concept for single low-energy phonons based on the quantum sensing of the spin of $^3$He atoms which have been evaporated from the surface of a He van der Waals film coating and ionic crystal. This is related to earlier proposals based upon He quantum evaporation [7, 12], though here we consider $^3$He which is bound to a $^4$He surface with an energy of ∼5 K [13], somewhat less than the ∼7 K binding of a $^4$He atom. More importantly, the nuclear spin of $^3$He allows its quantum sensing at the level of single atoms.

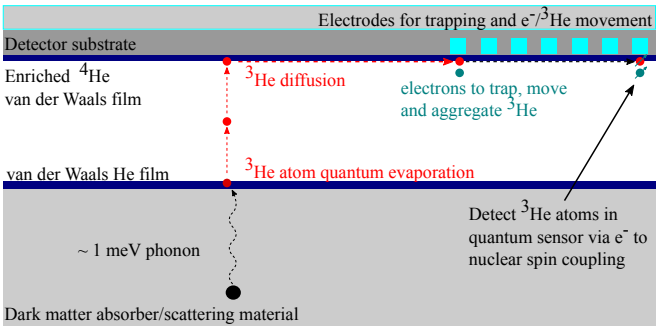


FIG. 1. Schematic of the DM detector concept. An interaction with DM in an ionic crystal generates ∼1 meV phonons, which impinge on a surface covered with a van der Waals helium film. The phonon quantum evaporates a $^3$He atom from the surface of the film, which is then collected on the van der Waals film covering the detector structures. The $^3$He atoms diffuse until captured by an electron bound to the helium surface in a CCD-like structure. Periodically the collected $^3$He atoms are moved with the CCD to a readout device which operates via nuclear spin induced decoherence of an electron in a spin based quantum sensor.

A diagram of this concept is shown in Fig. 1. There are four major steps in the dark matter detector proposed here and shown in the Figure: (1) production of phonons through the interaction with dark matter leading to the quantum evaporation of $^3$He atoms from Andreev bound states [14]; (2) trapping the $^3$He on the detector surface using electrons bound to a film of isotopically enriched liquid $^4$He; (3) collecting and transporting the electrons and trapped $^3$He atoms to a detector structure; and (4) quantum sensing of the $^3$He atoms through their nuclear spin. An important feature of this detection concept is the separation of the dark matter absorber (*i.e.* target,

such as a polar material) and the $^3$He detector, which opens the possibility to readily select and test a series of absorber materials for specific dark matter searches. Further, this approach is compatible with large magnetic fields, a feature that again enables testing of specific modes of proposed dark matter interactions. In addition, the disk-like form factor of the absorber-sensor package that we envision as shown schematically in Fig. 1 might enable future adaptation of our concept using similar device integration concepts as developed *e.g.* in SuperCDMS. In the remainder of this paper, we describe each of the steps of our detector concept in detail. It spans a range of fields, including dark matter astrophysics, solid state physics for phonon propagation, quantum fluids for $^3$He evaporation, device physics for $^3$He trapping and transport, and quantum information and sensing for $^3$He detection. Here we show how it can be a viable complement to existing efforts for light DM detection with TESs, SNSPDs, and CCDs.

*Helium evaporation via DM-produced phonons* — *Bulk* superfluid He has been proposed for DM detection through the production of phonons and rotons [7, 12]. By contrast, here we propose to use the helium as a means to detect the phonons produced in a solid target, and not as the target itself. This approach was also discussed in Ref. [12], though here we are specifically suggesting *polar* targets, such as NaI. Except for evidence that rotons do not efficiently evaporate $^3$He [15], the remainder of this approach to detecting low-energy DM interactions could be utilized for bulk He. However, there are important advantages and complementary opportunities to interacting and generating phonons in crystals (notably reach to a broader range of dark matter theories and masses [8, 9]), when evaporating $^3$He from these. We will focus on the case that a DM particle produces a single high-energy ($\gtrsim 10$ meV) phonon by an interaction with an ion in a polar material target. The anticipated DM interaction rate is about 2/min. in a 1 kg NaI crystal (detailed theoretical calculations can be found in Refs. [8, 9]), with an expected background from radioactive and cosmogenic species about 50 times lower. The appendices, include more detailed discussions of (1) detector crystal criteria, interaction rates, and backgrounds (2) other $^3$He detection approaches, and (3) possible alternative adsorbates.

Below about 80 mK a He surface is covered with $^3$He, both for bulk He and a van der Waals film. The athermal acoustic phonons resulting from the decay of the high-energy phonon, when interacting with the surface of the polar crystal coated with a thin helium film, can lead to quantum evaporation. Heat pulse experiments with natural abundance He films on crystalline substrates have shown that about 5% of the detected atoms are directly evaporated by phonons from the heat pulse – the "phonoatomic" effect depicted in Fig. 1, while the remainder are evaporated by the overall temperature rise of the crystal [16, 17]. However, these experiments have mostly used polished, rather than vacuum-cleaved surfaces. It is known that even well-polished surfaces covered with helium lead to enhanced phonon thermalization [18] and inefficient transport of phonons across the interface into a film [19]. The efficiency of quantum evaporation from a van der Waals film of liquid helium on a freshly cleaved surface which has been protected from oxygen and humidity is not known. Boosting the evaporation efficiency may also be possible by depositing a thin film of Cs on a crystal and coating that with a monolayer of $^3$He, as suggested in Ref. [17], since $^3$He is bound to Cs by only about 2.4 K.

*$^3$Helium trapping* — As shown in Fig. 1, the evaporated $^3$He atoms will be collected on an adjacent helium-covered surface. The helium in this collector film will be isotopically enriched to remove its $^3$He. Enrichment of $^4$He to less than 5 parts in $10^{13}$ ($< 0.5$ ppt) $^3$He has been demonstrated [20]. The enriched $^4$He film on this collector structure must be fully isolated from the $^3$He/$^4$He mixture coating the DM target crystal. There are two well-established approaches to breaking a van der Waals film: a film-burner as was employed in the HERON experiment [21]; and a band of cold-evaporated Cs, since superfluid $^4$He does not wet Cs [22, 23]. Here we expect that the Cs film will be preferable, since the film-burner could preferentially evaporate $^3$He atoms, which would appear as false events. After being captured onto this enriched $^4$He film, the $^3$He atoms diffuse across the film surface [24]. Our concept uses electrons held a few nanometers above the surface of the helium film by applied electric fields to localize $^3$He atoms in dimples under the electrons [25] and enable their transport to spin readout sensors for detection. It is essential that the $^3$He atoms be localized in the dimples for spin based $^3$He sensing, since if the $^3$He atoms are allowed to diffuse freely, motional narrowing causes them to have little effect on an electron's spin in a quantum sensor [26].

Trapping $^3$He in dimples under electrons bound to superfluid $^4$He is newly suggested here, and arises from $^3$He reducing the surface tension at mK temperatures [14]. The addition of a $^3$He atom will deepen the dimple, lowering the electron in the applied electric field, increasing its potential energy and trapping the $^3$He. The depth and shape of the dimple in the He surface will be determined by the equilibrium between electrostatic forces pulling the electron against the helium and capillary forces resisting the deformation.

To understand the temperature needed for stable trapping of the $^3$He we have performed numerical calculations of the helium dimple as shown in Fig. 2. These devices will use "channel" technology [27, 28] in which an underlying metal layer is first deposited on a substrate and patterned to make gate electrodes, and this layer of electrodes is then covered with an insulator and a second metallic layer. This upper metal layer is patterned lithographically, and areas are removed to form the channels where the electrons will reside. With a small amount of bulk superfluid, the helium covers the device through capillary action and fills the channels. Electrons emitted from the vacuum with a positive bias on the underlying gate electrodes accumulate on the helium film in the channels.

Fig. 2 shows calculated electrostatic potentials for a 200 nm wide channel that is 110 nm deep. The lower metal electrode is biased to +20 V, and the upper metal is at ground (0 V), with the potential contours at 1 V steps. The change in the dimple with the addition of a $^3$He atom is too small to be

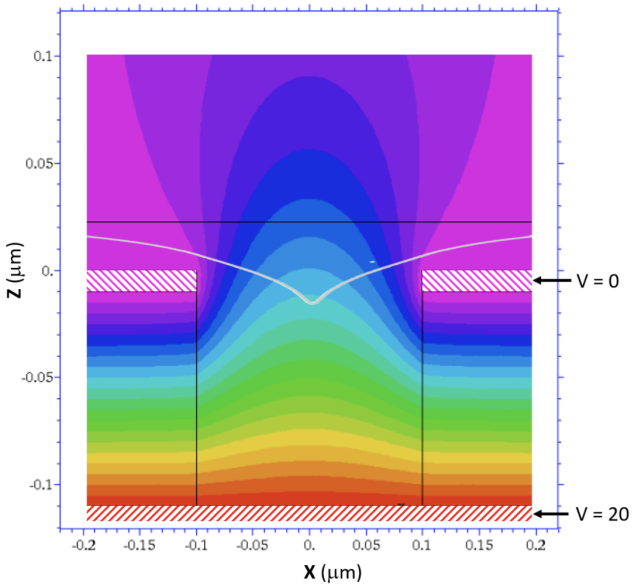


FIG. 2. Finite element calculation of the potential in a 0.2 $u$m wide He-filled channel with metal gates biased as shown. The channel is assumed to extend in the Y-direction (into the page) and electrons are placed with a periodicity of 0.2 $u$m. The contours are at 1 V steps. The black horizontal line at a height of ∼0.02 $u$m shows the helium surface without the electron or electric fields. The white curve superimposed on the potential image is the calculated helium surface for an electron held in the channel with the applied voltages.

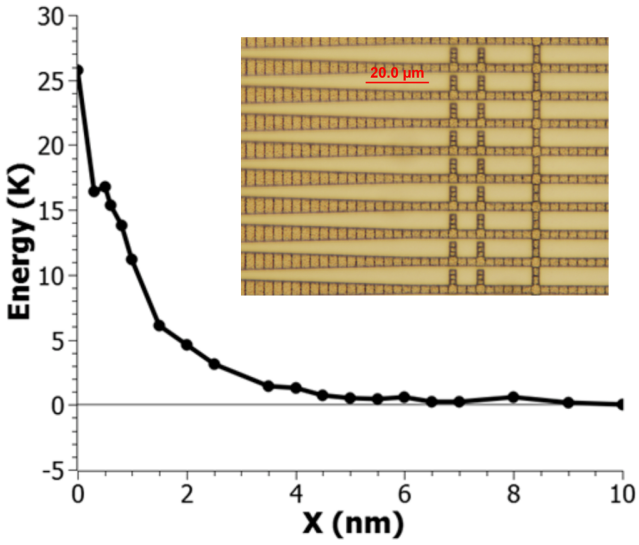


FIG. 3. Calculation of the binding energy of a $^3$He atom to an electron in a channel like that shown in Fig. 3, but with the $^3$He displaced by a distance (X) in the X-direction (across the channel). Lines connecting dots are guides to the eye. The inset shows a CCD used for moving electrons along helium filled channels (the micrograph shows the metal layers). The main channels run horizontally and are similar, though wider and deeper, to the CCDs needed for the detectors. The underlying gate electrodes run vertically as seen at the bottoms of the channels. (After Ref. [29])

seen in the figure, but the vertical electric field is calculated to be about $0.8 \times 10^6\,\mathrm{V\,cm^{-1}}$ at the electron, so a very small change in dimple depth can produce a significant change in electrostatic energy. For the parameters of Fig. 2, the calculated energy change per $^3$He atom is about 27 K. A variety of channel geometries and applied voltages have been modeled: higher voltages are required for narrow channels where capillary forces are stronger, while the helium surface becomes unstable if the channel becomes too wide. The calculations suggest that stable trapping of $^3$He is possible over at least a factor of 4 range in channel widths.

It is expected that this detector will be operated at ∼ 35 mK, or colder, since the background pressure of $^3$He must be kept very low. At this temperature, if the trapping energy is 2 K, the calculated density of free $^3$He atoms is $\sim 10^{-12}\,\mathrm{cm^{-2}}$ for every trapped $^3$He atom. Thus, trapping energies in the range of 1–2 K will be sufficient for localizing the $^3$He atoms.

Another consideration is the cross section for an electron to capture a $^3$He atom. Again, we have calculated the cross section numerically, here by introducing a change in the surface tension some distance from the electron to determine how the energy changes. Results for these same parameters (0.2 μm channel with a 20 V bias) are shown in Fig. 3. Taking the criterion for capture that the energy falls below kT, then we have a capture distance of ∼ 6 nm. In the orthogonal (Y) direction, calculations show that the capture distance is smaller, of order 1 nm. This can be readily understood, since the surface curvature is large in the X-direction, where van der Waals forces require the helium surface to bend tightly around the edges of the channel, as seen in Fig. 2. In the Y-direction the channel is long, the dimple is more gradual, and the change in surface tension is only felt very close to the electron.

The $^3$He forms a Fermi gas on the $^4$He surface at low densities, and its motion is diffusive. Measurements of the spin diffusion at low coverage (∼ 0.1 monolayers) in high surface area substrates finds a diffusivity of about $0.015\,\mathrm{cm^2\,s^{-1}}$ at 40 mK [30]. These measurements had 5 monolayers of $^4$He below the $^3$He, which is sufficient to be a superfluid and avoid localizing the $^3$He atoms. For simplicity we can approximate the capture perimeter as an ellipse with a minor axis of 1 nm and major axis of 6 nm and determine an effective isotropic capture cross section [31]. Assuming electrons are spaced 0.2 μm in Y, and the channels are spaced 0.2 μm in X (so electrons are 0.4 μm apart), we use this electron (trap) density, the capture cross section, and thermal velocity to calculate a capture time of about 100 ns and a diffusion length of about 1 μm. Thus, a reasonable density of electrons can rapidly capture the $^3$He, and the location of where the $^3$He arrived can be determined with a few micron accuracy. Micron-level resolution is unlikely to be necessary, and a lower density of channels and electrons should be adequate. For example, if the electrons are spaced 100 μm apart in both X and Y, the capture time for a $^3$He atom becomes about 0.1 s, and the spatial resolution is about 0.4 mm.

*$^3$Helium transport* — An important feature of this detector concept is the ability to collect $^3$He atoms over a large area and bring them to one or a few optimized quantum sensors. As discussed earlier, phonons are created in the bulk of a detector crystal, and they rapidly disperse the energy throughout the volume of the material, making their direct detection challenging. Our concept uses CCDs for $^3$He transport. In the inset of Fig. 3 we show a CCD which has been used to demonstrate essentially perfect charge-transfer efficiency [29] for electrons bound to helium. In this device the channels run horizontally, while the gate electrodes can be seen running vertically under the channels. As the gate voltages are controlled to move the electrons, they will drag the $^3$He atoms along with them in moving dimples. The CCD device in the inset of Fig. 3 was made at a standard silicon processing facility, which can fabricate similar electrode structures over large areas. The assumed 1 kg NaI crystal forms a disk about 2 cm thick and 13 cm in diameter, and thus the collector must be similar in size. Silicon devices with areas in that range are practical. Either a single large device could be fabricated, or a number of smaller ones can be tiled together, as is done for large-area optical CCDs. A variety of experiments have been performed with similar channel structures, including isolating individual and pairs of electrons [32, 33].

*$^3$He Detection* — After $^3$He atoms have been evaporated, captured, and collected with the CCD, it is necessary to detect single atoms. An electron's spin without a $^3$He trapped in the dimple below it is expected to have long phase coherence, since the spin-orbit interaction for an electron in the vacuum is particularly small [26]. However, if a $^3$He atom is trapped by an electron, the nuclear spin will rapidly decohere the spin of an electron initially prepared in a superposition of up and down spin. This decoherence will happen in less than a 1 ms, while the spin coherence of electrons bound to helium is thought to be at least seconds [26]. This is a quantum nondemolition process and can be repeated as long as the $^3$He remains trapped, allowing multiple interrogations to ensure reliable detection. Several approaches to detecting the spin of single electrons bound to helium are under active investigation, driven by quantum computing applications, and are discussed in the Appendix. Once the measurement is complete, any detected $^3$He atoms will be clocked with the CCD to a region with a large number of electrons tightly bound in circular ($\sim$200 nm diameter) "quantum dots". The $^3$He atoms will be trapped and gettered by these electrons. Residual $^3$He atoms present when the detector is initialized will similarly be collected and moved to the getter region with the CCD. A 100 nm thick enriched He layer over the collector area (for the 13 cm diameter target) can be expected to have $\sim 10^7$ $^3$He atoms, but it is quite straightforward to fabricate $10^8$ or more quantum dots in an area of $\sim$10 mm$^2$, and each dot can trap multiple $^3$He atoms.

As noted above, a cursory evaluation of detector crystals suggests that NaI may be appropriate. The estimate of 2 DM scattering events/minute, with the probability of detecting an event being about 35%, compares favorably with the most important expected background dominated by $^{40}$K decays which will occur about about once per hour. More detail about the expected detector backgrounds is discussed in the Appendix. The generation of scintillation photons as well as large numbers of phonons in one area in a short time can be used as a veto for high energy events, such as radioactive decays and Compton scattering. The frequency of readout operation cycles with $^3$He collection, quantum sensing, and $^3$He gettering will be adjusted to match event and background rates. Readout times of a few ms are slow, on the typical scale of CCDs and electronics, and thus the heat load is expected to be small enough to allow operation at 35 mK, or colder. The heat load could be further reduced with superconducting metallization on the $^3$He detector structure, though this is probably unnecessary since nearly all the power will be dissipated in driver circuitry at higher temperature.

*Summary* — In summary we have presented a new concept for detecting low energy ($\sim$meV) excitations, in particular those which might be generated in target materials through the interaction with low-mass dark matter. The approach begins with a DM interaction producing phonons in an ionic crystal, which cause the quantum evaporation of $^3$He from the surface. The $^3$He is then caught on an adjacent surface, where there is an isotopically enriched van der Waals $^4$He film covering a layer of metallic electrodes and etched microchannels holding electrons on the film. We calculate that the electrons on liquid helium can trap the $^3$He atoms, and they will drag $^3$He atoms as they are clocked across the helium surface in a CCD, allowing $^3$He atoms to be collected for detection by quantum sensors. We suggest that the spin of $^3$He atoms can be coupled to electron spins for sensitive detection — to the level of a single $^3$He atom. Thus the difficult balance of efficient detection of very rare low-energy events occurring throughout a large volume is solved in our approach through the trapping, collection, and quantum sensing of the $^3$He atoms. Calculations of dark photon mediated interactions and estimates of the various background processes show that with a kg-sized ionic crystal a detected DM event rate of about 40/hr can be achievable, while high-energy radioactive decays and Compton events will be about 50 times less frequent. These high-energy events can be distinguished by the detector, and thus vetoed. Coherent photon and neutrino scattering will produce low-energy events, similar to DM, but their estimated rates are over 3 orders of magnitude less than the DM. Assemblies of dark matter sensors of this design could operate for long periods with periodic readout of accumulated $^3$He atoms

All major aspects of this detector concept are based on established experimental results, or in the cases of single spin measurement and $^3$He trapping (also suggested for electron bubbles [34]), they are being actively pursued in the context of quantum computer development with electrons on liquid helium [26]. Experimental verification of spin measurement and $^3$He trapping will enable first-generation detectors and open the door to this path of quantum sensing of phonons for DM detection.

## ACKNOWLEDGMENTS

This work was supported by Quantum Information Science Enabled Discovery (QuantISED) for High Energy Physics and by the Office of Science of the U.S. Department of Energy under Contract No. DE-AC02-05CH11231.


## APPENDICES

*Appendix 1. Detector Crystal and Background* — An initial phonon with an energy of a few 10s of meV created in a dark matter scattering event typically decays through a sequence of inelastic processes to acoustic phonons with frequencies of order 1 THz, where thermalization is slowed in high-quality crystals by the decreasing phonon density of states. [35] We will consider light DM detection by a 1 kg NaI crystal with $^3$He quantum sensing of the resulting phonons. Other crystals may prove to be superior, but from a cursory look NaI satisfies several criteria: (1) it has low energy cut-off ($\sim$20 meV) for phonons generated by DM [8]; (2) it can be purified to have a low radioactive background; (3) neither Na nor I have multiple naturally occurring isotopes, thus eliminating isotopic scattering of the acoustic phonons; and (4) it can be cleaved, which will reduce the phonon thermalization at surfaces and may increase the yield of evaporated $^3$He atoms. From calculations of the cross section for DM interaction within a dark photon interaction model and a freeze-in model of the DM flux [9], one finds that the rate of DM events is about 2/minute at a DM mass of about 20 keV in 1 kg of NaI with a minimum energy cut-off of 20 meV. A 20 meV phonon in the NaI will decay to about 20 acoustic phonons with enough energy to quantum evaporate the $^3$He. If we assume that the efficiency for an acoustic phonon to desorb a helium atom is $\sim 5\%$ [16, 17], and the probability of that atom being a $^3$He is about 1/3 [15], there is thus about a 1/60 chance of a single acoustic phonon being detected through $^3$He evaporation. With each DM event producing $\sim$20 acoustic phonons, we estimate about one $^3$He atom will be produced every 1.5 minutes. Improved preparation of the NaI surfaces or better ionic crystals may increase the $^3$He evaporation rate.

Backgrounds for this detector are expected to be similar to those seen by other DM experiments. The DAMA/LIBRA and KIMS experiments [36, 37]) have established that an important background source in NaI is residual $^{40}$K. Large NaI crystals with no more than 20 ppb of potassium impurities [36] imply a decay rate of about 1.2/kg/hr. The decay of cosmogenic tritium will also contribute to the background. The CDMSlite experiment [38] has found a tritium production rate of $\sim$75 atoms/kg/day in a Ge detector. Calculations of the tritium production for NaI find a rate of about 83 atoms/kg/day at sea level. [39] Assuming 60 says at sea level for detector crystal preparation before installation underground, the cosmogenic tritium will contribute about one decay every 30 hours. Each decay of $^{40}$K and tritium will generate many phonons and thus many $^3$He atoms. If the detector is read out more frequently than these background events, the large signals can be used as a veto. These high energy events will also produce scintillation photons which can provide another avenue for vetoing them. Taken together it is anticipate that there will be about 50 detectable DM events between $^{40}$K and tritium decays under the assumptions discussed above. Since these decays can be vetoed based on their deposited energy, they will contribute to detector dead time, but will not otherwise interfere with the DM signal. Compton scattering of MeV-scale photons will deposit high energies in the detector crystal, which can be vetoed as described above, but Robinson has pointed out that coherent photon scattering can deposit much smaller energies, of the same order as DM events. [40] He has calculated an integrated scattering rate of $\sim$0.34 events/kg/day for recoil energies below 1 eV in Ge, assuming a well-constructed passive radiation shield and neglecting both coherence between atoms and phonon quantization in the crystal. Again, higher energy events can be vetoed. The iodine in the NaI crystal will dominate the coherent photon scattering, having a 3.8x larger atomic cross section than Ge through the relevant energy range [41]. Under similar assumptions we estimate that coherent photon scattering will produce $\sim$0.6 recoils/kg/day. Being of similar energy as the DM events, it is not possible to veto these recoils, but their rate is about 3 orders of magnitude lower than the calculated DM rate (2/kg/min. in NaI). Coherent neutrino scattering will similarly generate recoils which cannot be vetoed based on deposited energy. However, for recoil energies below $\sim$1 eV, the coherent photon scattering rates as estimated by Robinson exceed the expected coherent neutrino rates. [40, 42] Thus, while the photons and neutrinos will add a small offset to the DM signal, this background is expected to be smaller by several orders of magnitude.

The collector device can also introduce backgrounds from radioactive decay. It appears best to avoid Al metallization in the collector chip, since cosmogenic $^{26}$Al could add a considerable background. A copper process will avoid this issue. If the collector is made as a standard silicon device, it will also introduce signals from the decay of cosmogenic $^{32}$Si, as has been seen in other DM experiments. The DAMIC experiment [43] has quantified the radioactivity of $^{32}$Si, and finds it contributes about 80 decays/kg/day. A typical Si wafer with the 13 cm diameter discussed above weighs about 30 gm, and thus the $^{32}$Si can be expected to cause about 3 events/day. Again, these are high energy events which can be vetoed. Being considerably lighter than the target crystal, the tritium background from the collector is not expected to be a major contributor, with a rate comparable to $^{32}$Si.

Other background sources for this class of quantum evaporation detectors have been identified and modeled as part of the HeRALD experiment, [7] including the layers of shielding required. Background excitation of the helium is suppressed by its large bandgap for electronic excitations. NaI has a smaller gap, of about 5.8 eV, but most of that analysis carries over to this case. The gap still protects against low-energy processes. If an event does excite an electron across the gap, a large number of phonons will be produced when

the electron-hole pair recombine or are trapped, and again these events can be identified. There is evidence in some other ultra-sensitive DM detection devices that stresses built up in materials can slowly relax by emitting phonons. In the detectors discussed here no thin films are deposited on the target crystals. Such films can undergo thermal expansion mismatch stresses, though low-stress mounting will still be important.

*Appendix 2. $^3$He Detection* — Multiple approaches are being taken by different groups for measuring spins on helium. Detection of single nuclear spins in other systems has been accomplished with quantum sensors in recent years. For example, nitrogen-vacancy centers have been used to sense the presence of nearby $^{29}$Si atoms [44]. However, it is not clear whether direct nuclear spin detection can be adapted to the situation of a $^3$He atom on $^4$He, since the direct sensing of nuclear spins has relied on extremely close and stable positioning of the nucleus and the sensor. Converting to an electron spin, with its much larger magnetic moment, appears easier as discussed in the main text. Detection of single electron spins has been demonstrated in a range of quantum sensor and qubit platforms, from quantum dots to color centers [45]. It has been shown that the electron motion can be coupled to a superconducting resonator with a coupling constant of $\sim 5\,$MHz [46]. However, these first experiments were limited by decoherence of the motional states, apparently due to vibrations exciting fluctuations in the helium surface. Recently, strong coupling of the electron motion to a superconducting micro-resonator while bound to solid neon has been demonstrated [47]. Isolating the helium from the vibrations is being investigated in several labs and a high degree of vibration isolation will be central to the integration of our detector concept. With the motion strongly coupled to the resonator, an inhomogeneous magnetic field can provide the spin interaction, as has been demonstrated for electrons in silicon quantum dots [48, 49]. In an alternative configuration, one could utilize a pair of electrons initialized to a spin singlet in a nanofabricated quantum dot, separating the two electrons, trapping the $^3$He under one to shift its phase, and then bringing the electrons back together to determine whether they are still a singlet. Decoherence from (single) $^3$He atoms will drive them from the singlet to the triplet with $m = 0$. A third approach would be to use a color center, like a $NV^-$ or $SiV^0$ in diamond to sense the electron spin (much less demanding than sensing a nuclear spin) [50]. Direct ESR techniques may also be possible, where sensitivity to a single electron's spin has recently been demonstrated. [51] The signal could be enhanced by using one $^3$He atom to sequentially decohere multiple electrons, since the atom is preserved in the process (its spin need not be preserved).

Here we have concentrated on using the $^3$He nuclear spin for quantum sensing, but there may be other ways to utilize the unique signatures of $^3$He. For example, the CCDs could be arranged to transport all of the $^3$He atoms to one place, where they are ejected from the surface with a heat pulse. With the atoms all emerging in one place, an ionization process like that described by Maris, *et al.* [12], but with isotope-selective (perhaps optical) excitation, could be employed. Alternatively, ultra-sensitive mass spectrometry or other sensing technique might be enabled with the localized He source.

*Appendix 3. Alternative Adsorbates* — We have concentrated on the evaporation of $^3$He from the surface of liquid $^4$He, since it has the lowest surface binding energy ($\sim 5\,$K). However, many other atomic and molecular species as well as electrons can be bound to a liquid He surface, and their evaporation may prove useful as phonon detectors. An isolated electron binds with an energy of $\sim 0.6\,$meV [52], but a high electron density is necessary if the ejection of an electron is to have a high probability. However, large holding fields are then required to hold the electrons on the surface, and electron emission is limited by electron-electron interactions [53]. Alkali metals were predicted to bind to helium with energies of $10 \sim 20\,$K [54], and experimentally found to bind to the surface of He nanodroplets [55]. Being uncharged they do not require holding fields, but at high densities they form dimers and clusters. It has also been reported that other species, such as HD, can be desorbed from alkali halides with a single phonon [56]. Such species may be useful as detectors for particular energy ranges of proposed dark matter candidates and interactions. Being much more polarizable than He, it may also be possible to tune their desorption energy with an applied electric field.

* Current address: Honeywell Corp. Minneapolis, MN 55422


[1] P. Cushman *et al.*, in *Community Summer Study 2013: Snowmass on the Mississippi* (2013) arXiv:1310.8327 [hep-ex].

[2] M. Battaglieri *et al.*, in *U.S. Cosmic Visions: New Ideas in Dark Matter* (2017) arXiv:1707.04591 [hep-ph].

[3] L. Barak, I. M. Bloch, M. Cababie, G. Cancelo, L. Chaplinsky, F. Chierchie, M. Crisler, A. Drlica-Wagner, R. Essig, J. Estrada, E. Etzion, G. F. Moroni, D. Gift, S. Munagavalasa, A. Orly, D. Rodrigues, A. Singal, M. S. Haro, L. Stefanazzi, J. Tiffenberg, S. Uemura, T. Volansky, and T.-T. Yu (SENSEI Collaboration), Phys. Rev. Lett. **125**, 171802 (2020).

[4] I. Alkhatib *et al.* (SuperCDMS), Phys. Rev. Lett. **127**, 061801 (2021), arXiv:2007.14289 [hep-ex].

[5] S. Knapen, T. Lin, M. Pyle, and K. M. Zurek, Phys. Lett. **B785**, 386 (2018), arXiv:1712.06598 [hep-ph].

[6] K. Schutz and K. M. Zurek, (2016), arXiv:1604.08206 [hep-ph].

[7] S. A. Hertel, A. Biekert, J. Lin, V. Velan, and D. N. McKinsey, Phys. Rev. D **100**, 092007 (2019).

[8] T. Trickle, Z. Zhang, K. M. Zurek, K. Inzani, and S. M. Griffin, JHEP **03**, 036 (2020), arXiv:1910.08092 [hep-ph].

[9] S. M. Griffin, K. Inzani, T. Trickle, Z. Zhang, and K. M. Zurek, Phys. Rev. D **101**, 055004 (2020).

[10] A. Mitridate, T. Trickle, Z. Zhang, and K. M. Zurek, Phys. Rev. D **102**, 095005 (2020).

[11] Y. Hochberg, M. Pyle, Y. Zhao, and K. M. Zurek, JHEP **08**, 057 (2016), arXiv:1512.04533 [hep-ph].

[12] H. J. Maris, G. M. Seidel, and D. Stein, Phys. Rev. Lett. **119**, 181303 (2017).

[13] D. . Edwards and W. F. Saam, Prog. Low Temp. Phys. **7A**, 284 (1978).

[14] A. F. Andreev, Zhurnal Eksperimental'noi i Teoreticheskoi Fiziki (U.S.S.R.) For English translation see Sov. Phys. - JETP (Engl. Transl.) **50** (1966).

[15] J. P. Warren and C. D. Williams, Physica B **284-288**, 160 (2000).

[16] D. L. Goodstein, R. Maboudian, F. Scaramuzzi, M. Sinvani, and G. Vidali, Phys. Rev. Lett. **54**, 2034 (1985).

[17] T. More, J. S. Adams, S. R. Bandler, S. M. Brouër, R. E. Lanou, H. J. Maris, and G. M. Seidel, Phys. Rev. B **54**, 534 (1996).

[18] F. Türk, G. Ullrich, and H. Kinder, Ann. Phys. **507**, 165 (1995).

[19] C. H. Anderson and E. S. Sabisky, Phys. Rev. Lett. **24**, 1049 (1970).

[20] P. Hendry and P. McClintock, Cryogenics **27**, 131 (1987).

[21] R. Torii, S. R. Bandler, T. More, F. S. Porter, R. E. Lanou, H. J. Maris, and G. M. Seidel, Review of Scientific Instruments **63**, 230 (1992).

[22] P. J. Nacher and J. Dupont-Roc, Phys. Rev. Lett. **67**, 2966 (1991).

[23] P. Taborek and J. E. Rutledge, Phys. Rev. Lett. **68**, 2184 (1992).

[24] P. A. Sheldon and R. B. Hallock, Phys. Rev. Lett. **77**, 2973 (1996).

[25] R. Williams and R. Crandall, Phys. Lett. A **36**, 35 (1971).

[26] S. A. Lyon, Phys. Rev. A **74**, 052338 (2006).

[27] D. Marty, J. Phys. C **19**, 6097 (1986).

[28] R. van Haren, G. Acres, P. Fozooni, A. Kristensen, M. Lea, P. Richardson, A. Valkering, and R. van der Heijden, Physica B **249-251**, 656 (1998).

[29] F. R. Bradbury, M. Takita, T. M. Gurrieri, K. J. Wilkel, K. Eng, M. S. Carroll, and S. A. Lyon, Phys. Rev. Lett. **107**, 266803 (2011).

[30] P. A. Sheldon and R. B. Hallock, Phys. Rev. Lett. **85**, 1468 (2000).

[31] C. R. Crowell, Appl. Phys. **9**, 79 (1976).

[32] G. Papageorgiou, P. Glasson, K. Harrabi, V. Antonov, E. Collin, P. Fozooni, P. G. Frayne, M. J. Lea, D. G. Rees, and Y. Mukharsky, Appl. Phys. Lett. **86**, 153106 (2005).

[33] M. Takita and S. A. Lyon, J. Phys: Conf. Ser. **568**, 052034 (2014).

[34] A. J. Dahm, Phys. Rev. **180**, 259 (1969).

[35] J. P. Wolfe, *Imaging Phonons: Acoustic Wave Propagation in Solids* (Cambridge University Press, 1998).

[36] R. Bernabei, P. Belli, A. Bussolotti, F. Cappella, R. Cerulli, C. Dai, A. d'Angelo, H. He, A. Incicchitti, H. Kuang, J. Ma, A. Mattei, F. Montecchia, F. Nozzoli, D. Prosperi, X. Sheng, and Z. Ye, (2008), arXiv:0804.2738 [astro-ph].

[37] G. Adhikari, P. Adhikari, C. Ha, E. Jeona, N. Kim, Y. Kim, S. Kong, H. Lee, S. Oh, J. Park, and K. Park, (2017), arXiv:1703.01982v3 [astro-ph].

[38] R. Agnese, T. Aralis, T. Aramaki, I. Arnquist, E. Azadbakht, W. Baker, S. Banik, D. Barker, D. Bauer, T. Binder, M. Bowles, P. Brink, R. Bunker, B. Cabrera, R. Calkins, C. Cartaro, D. Cerdeño, Y.-Y. Chang, J. Cooley, B. Cornell, P. Cushman, T. Doughty, E. Fascione, E. Figueroa-Feliciano, C. Fink, M. Fritts, G. Gerbier, R. Germond, M. Ghaith, S. Golwala, H. Harris, Z. Hong, E. Hoppe, L. Hsu, M. Huber, V. Iyer, D. Jardin, A. Jastram, C. Jena, M. Kelsey, A. Kennedy, A. Kubik, N. Kurinsky, R. Lawrence, B. Loer, E. Lopez Asamar, P. Lukens, D. MacDonell, R. Mahapatra, V. Mandic, N. Mast, E. Miller, N. Mirabolfathi, B. Mohanty, J. Morales Mendoza, J. Nelson, J. Orrell, S. Oser, W. Page, R. Partridge, M. Pepin, F. Ponce, S. Poudel, M. Pyle, H. Qiu, W. Rau, A. Reisetter, R. Ren, T. Reynolds, A. Roberts, A. Robinson, H. Rogers, T. Saab, B. Sadoulet, J. Sander, A. Scarff, R. Schnee, S. Scorza, K. Senapati, B. Serfass, D. Speller, M. Stein, J. Street, H. Tanaka, D. Toback, R. Underwood, A. Villano, B. von Krosigk, S. Watkins, J. Wilson, M. Wilson, J. Winchell, D. Wright, S. Yellin, B. Young, X. Zhang, and X. Zhao, Astroparticle Physics **104**, 1 (2019).

[39] J. Amare, J. Castel, S. Cebrian, I. Coarasa, C. Cuesta, T. Dafni, J. Galan, E. Garcıa, J. Garza, F. Iguaz, I. Irastorza, G. Luzon, M. Martınez, H. Mirallas, M. Olivan, Y. Ortigoza, A. Ortiz de Solorzano, J. Puimedon, E. Ruiz-Choliz, M. Sarsa, J. Villar, and P. Villar, (2017), arXiv:1706.05818 [physics.ins-det].

[40] A. E. Robinson, arXiv:1610.07656v4 [astro-ph].

[41] B. K. Chatterjee and S. C. Roy, J. Phys. Chem. Ref. Data **27**, 1011 (1998).

[42] J. Billard, E. Figueroa-Feliciano, and L. Strigari, Phys. Rev. D **89**, 023524 (2014).

[43] A. Aguilar-Arevalo, D. Amidei, X. Bertou, D. Bole, M. Butner, G. Cancelo, A. C. Vázquez, A. Chavarria, J. de Mello Neto, S. Dixon, J. D'Olivo, J. Estrada, G. F. Moroni, K. H. Torres, F. Izraelevitch, A. Kavner, B. Kilminster, I. Lawson, J. Liao, M. López, J. Molina, G. Moreno-Granados, J. Pena, P. Privitera, Y. Sarkis, V. Scarpine, T. Schwarz, M. S. Haro, J. Tiffenberg, D. T. Machado, F. Trillaud, X. You, and J. Zhou, J. Instr. **10**, P08014 (2015).

[44] C. Müller, X. Kong1, J.-M. Cai, K. Melentijević, A. Stacey, M. Markham, D. Twitchen, J. Isoya, S. Pezzagna, J. Meijer, J. Du, M. Plenio, B. Naydenov, L. McGuinness, and F. Jelezko, Nat. Commun. **5**, 4703 (2014).

[45] C. L. Degen, F. Reinhard, and P. Cappellaro, Rev. Mod. Phys. **89**, 035002 (2017).

[46] G. Koolstra, G. Yang, and D. I. Schuster, Nature Commun. **10**, 5323 (2019).

[47] X. Zhou, G. Koolstra, X. Zhang, G. Yang, X. Han, B. Dizdar, D. Ralu, W. Guo, K. W. Murch, D. I. Schuster, and D. Jin, (2021), arXiv:2106.10326 [Quant-Ph].
[48] X. Mi, M. Benito, S. Putz, D. M. Zajac, J. M. Taylor, G. Burkard, and J. R. Petta, Nature **555**, 599 (2018).
[49] N. Samkharadze, G. Zheng, N. Kalhor, D. Brousse, A. Sammak, U. C. Mendes, A. Blais, G. Scappucci, and L. M. K. Vandersypen, Science **359**, 1123 (2018).
[50] J. M. Taylor, P. Cappellaro, L. Childress, L. Jiang, D. Budker, P. R. Hemmer, A. Yacoby, R. Walsworth, and M. D. Lukin, Nat. Phys. **4**, 810 (2008).
[51] Z. Wang, L. Balembois, M. Rančić, E. Billaud, M. L. Dantec, A. Ferrier, P. Goldner, S. Bertaina, T. Chanelière, D. Estève, D. Vion, P. Bertet, and E. Flurin, (2023), arXiv:2301.02653 [quant-ph].
[52] M. W. Cole, Rev. Mod. Phys. **46**, 451 (1974).
[53] K. Kono, K. Kajita, S.-i. Kobayashi, and W. Sasaki, J. Low Temp. Phys. **46**, 195 (1982).
[54] F. Ancilotto, E. Cheng, M. W. Cole, and F. Toigo, Z. Phys. B **98**, 323 (1995).
[55] F. Stienkemeier, J. Higgins, C. Callegari, S. I. Kanorsky, W. E. Ernst, and G. Scoles, Z. Phys. D **38**, 253 (1996).
[56] P. M. Ferm, S. R. Kurtz, K. A. Pearlstine, and G. M. McClelland, Phys. Rev. Lett. **58**, 2602 (1987).